Electronic Structure of Spinel-Type Nitride Compounds Si_3N_4, Ge_3N_4, and Sn_3N_4 with Tunable Band Gaps: Application to Light Emitting Diodes

T. D. Boyko,[1] A. Hunt,[1] A. Zerr,[2] and A. Moewes[1,*]

[1]*Department of Physics and Engineering Physics, University of Saskatchewan, 116 Science Place, Saskatoon, Saskatchewan S7N 5E2, Canada*

[2]*LSPM-CNRS, Université Paris-Nord, 99 avenue J. B. Clement, 93430 Villetaneuse, France*

(Received 9 June 2013; published 30 August 2013)

In this Letter using experimental and theoretical methods, we show that the solid solutions of group 14 nitrides having spinel structure (γ-M_3N_4 where M = Si, Ge, Sn) exhibit mainly direct electronic band gaps with values that span the entire visible wavelength region, making these hard and thermally stable materials suitable for optoelectronic devices and, in particular, lighting applications. Using the simulated band structure, we also calculate the exciton binding energy. The combination of large exciton binding energies and the tunable electronic band gaps in the visible range makes these binary spinel nitrides and their solid solutions a new class of multifunctional materials with optoelectronic properties that can be engineered to suit the desired application.

DOI: 10.1103/PhysRevLett.111.097402 PACS numbers: 78.70.En, 71.15.Mb, 71.35.−y, 78.70.Dm

Conventional lighting devices (incandescent and fluorescent) consume a large amount of energy and modern technologies such as light emitting diodes (LEDs) and phosphor converting-LEDs (pcLEDs) are used to decrease the global energy demand with regard to lighting. The most recent significant progress in this field was achieved by the development of blue and white LEDs [1]. While the efficiency, operational lifetime and robustness of LEDs exceed that of conventional light devices, the heat released in the diode junction needs to be efficiently managed and demands the use of materials that have high thermal stability. Many LEDs are based on binary or ternary compounds of groups 13 and 15 elements such as GaN, InN, GaAs, GaP, etc. [2], but these compounds have several disadvantages. They are relatively expensive since group 13 elements are rare, some are toxic (e.g., GaAs), and almost all are relatively inefficient due to their small exciton binding energies (E_b) [3,4]. They are also not stable against hydrolysis and oxidation in air, especially at elevated temperatures, and require a passivation layer reducing their overall efficiency.

Zinc oxide (ZnO) and hexagonal boron nitride (h-BN) are some alternative LED materials now under consideration. ZnO has a band gap (E_g) of ≈ 3.3 eV and a large exciton binding energy of $E_b = 60$ meV [5], but it degrades under humid atmosphere, and it is classified as dangerous for the environment. On the other hand, h-BN has a large band gap of $E_g \approx 6.0$ eV [6], but the efficiency is extremely sensitive to deformations, which induce considerable quenching of the exciton emission [7]. A new class of tunable materials is needed to continue the development of more efficient and robust lighting devices.

In this Letter, we investigate the electronic structure of the novel high-pressure nitrides of group 14 elements having a cubic spinel structure (γ-M_3N_4, where M = Si, Ge, Sn) [8–10]. These materials have a unique combination of mechanical, chemical, and electronic properties that make them highly advantageous [11–16] as alternative materials for the fabrication of LEDs when compared with (Ga,In)(As,N), ZnO, or h-BN. Specifically, these three spinel nitrides have direct electronic band gaps and will exhibit efficient conversion of electric power to light when used in LED devices, not accounting for the exciton binding energy which remains to be determined. Contrary to conventional LED materials (GaN, GaAs, etc.), γ-Si_3N_4 and γ-Ge_3N_4 remain stable in air when heated to temperatures of 1400 °C [17] and 700 °C [18], respectively, while γ-Sn_3N_4 remains stable in vacuum to at least 300 °C [10] as well as air to at least 200 °C [19], and thus, these materials do not require any passivation layer.

Initially, group 14 spinel nitrides were synthesized at high temperatures (800–1800 K) and pressures (12–23 GPa) in diamond anvil cells [8], multianvil cells [20,21], or through shock compression [22]. However, there has already been some success in depositing γ-Sn_3N_4 as a thin film, which is evident from the x-ray diffraction pattern [19,23]. Since γ-Sn_3N_4 is synthesized at ambient conditions and deposited as films, we expect that the entire γ-M_3N_4 materials class can be deposited as thin films similar to the related high-pressure c-Zr_3N_4, which shows excellent adhesion to a variety of substrates including silicon, glass, or cemented carbides [24]. With direct electronic band gaps as well as high thermal and oxidation stability, spinel nitrides are suitable for a variety of applications.

The work presented here has two overarching goals. Our first goal is to both measure and calculate the electronic band gaps as well as calculate the exciton binding energies of the three binary spinel nitrides, γ-Si_3N_4, γ-Ge_3N_4, and γ-Sn_3N_4. The expertise gleaned will allow us to realize our second goal: using density functional theory (DFT), we predict the electronic band gap of the solid solutions

γ-(Sn, Ge)$_3$N$_4$. As we shall show, the spinel-structured nitrides form a class of multifunctional compounds with easily tunable band gap values in the visible and near IR range, which is highly desirable in optoelectronics and lighting applications.

The N p states of binary spinel nitrides were chosen here to study the electronic structure of binary spinel nitrides for two reasons. First, our calculations show that the N p states are hybridized throughout the entire conduction band (CB) and valence band (VB), including the very top of the VB and the bottom of the CB. Thus, the N p states provide an accurate measure of the band gap with minimal multielectronic effects. Second, these compounds contain small amounts of oxygen substituting for nitrogen at the anion positions throughout the bulk of the material because the synthesis techniques used to make the materials studied here do not allow one to completely exclude oxygen diffusion in the reaction volume [10,20,25]. As such, the cation measurements would have a significant oxygen contribution and the N p states provide a probe of the electronic structure without any oxygen distortion.

The x-ray emission spectroscopy (XES) and x-ray absorption near edge structure (XANES) measurements were taken using synchrotron radiation at Beamline 8.0.1 (Advanced Light Source) [26] and Spherical Grating Monochromator beamline (Canadian Light Source) [27], respectively. The samples of γ-Si$_3$N$_4$ and γ-Ge$_3$N$_4$ were synthesized using a multianvil press, while γ-Sn$_3$N$_4$ was synthesized at ambient conditions. The synthesis and structural details of all three materials have been previously published [10,20,21]. The γ-Si$_3$N$_4$, γ-Ge$_3$N$_4$, and γ-Sn$_3$N$_4$ samples investigated in this work were a single polycrystalline piece, a polycrystalline powder, and another polycrystalline powder (10 vol. % of SnO_2 and 5 vol. % of SnO), respectively. Prior to the XES and XANES measurements, the γ-Si$_3$N$_4$ sample surface was dry polished on a diamond abrasive foil in a glove bag filled with nitrogen gas. The γ-Ge$_3$N$_4$ and γ-Sn$_3$N$_4$ samples, being both polycrystalline powders, were pressed into freshly scraped indium foil. These materials were affixed to the sample holder and oriented at 30° with respect to the incoming x-ray beam. Figure 1 shows the measured N $K\alpha$ XES and N 1s XANES spectra, which were calibrated using the same procedure described in Ref. [28].

The electronic band gap is the energy separation between the VB and CB states, which can be probed using XES and XANES measurements, respectively. The method used here to determine the band edges for the XES and XANES spectra is the second derivative method [28–30]. This technique has the advantage over conventional band gap determination methods in that it is much less sensitive to impurities and material defects due to the local nature of the measurements. However, it is not enough to simply measure the band gap; the final state of a XANES measurement has a core hole, which can distort the unoccupied density of states severely.

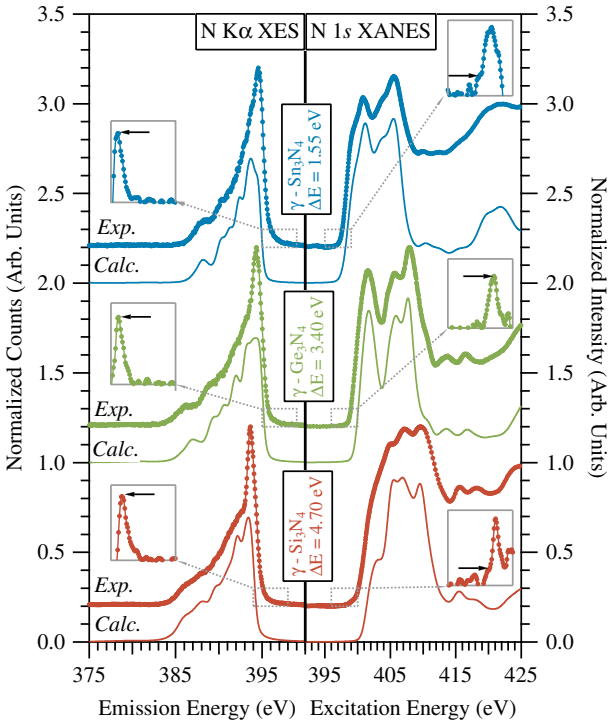

FIG. 1 (color online). The measured and calculated N $K\alpha$ XES and N 1s XANES spectra of γ-M_3N$_4$ (M = Si, Ge, Sn) are displayed. The second derivatives of the experimental spectra are displayed in the grey panel insets, with the regions displayed enclosed by the connected dashed box. The measured energy separation (excluding the core hole shift) between the measured band edges (ΔE) is labeled.

To quantify the core hole effect, we have performed both ground state and excited state DFT calculations, the latter with a core hole included. The relative difference in CB onsets between the ground and excited states allows one to arrive at a core hole shift (CH).

The XES and XANES spectra were simulated using the commercially available WIEN2K software package (ver. 11.1), an *ab initio* full potential DFT code [31]. These calculations used the generalized gradient approximation (GGA) functional of Perdew-Burke-Ernzerhof [32]. The XANES calculations used a $1 \times 2 \times 2$ supercell in order to adequately isolate the included core hole. The calculations here utilized the following parameters: $E_{cut} = -8.7$ Ryd, $Rk_{max} = 7.0$, and $E_{max} = 4.5$ Ryd. The k-point grids used were $10 \times 10 \times 10$ and $10 \times 5 \times 5$ for the XES and XANES calculations, respectively. The XANES calculations implemented the core hole effect by removing a full core electron and adding a uniform background charge of e. The XES and XANES calculations utilized a self-consistent field cycle with energy and charge convergence of 0.0001 Ryd and 0.001 e, respectively. Our DFT calculations reveal CH values of 0.1, 0.1, and 0.0 eV for γ-Si$_3$N$_4$, γ-Ge$_3$N$_4$, and γ-Sn$_3$N$_4$, respectively. Adding these CH corrections to the experimental band gaps results in true ground state band gap values of 4.8 ± 0.2,

3.5 ± 0.2, and 1.6 ± 0.2 eV for γ-Si_3N_4, γ-Ge_3N_4, and γ-Sn_3N_4, respectively.

The simulated XANES spectra (see Fig. 1) reproduce not only the general shape of the experimental spectra but also every spectral feature for all the examined binary spinel nitrides. This agreement suggests that the values of the CH shifts extracted from the DFT calculations are correct since the core hole must be included in order to simulate the measured N 1*s* XANES spectra. Further, the agreement between the simulated and measured spectra clearly shows that the materials are not contaminated with other N-containing materials. The values for γ-Si_3N_4 and γ-Ge_3N_4 have been determined previously through similar methods [28] and agree with the values presented here within experimental error, but the values presented here are a result of much higher quality XES and XANES measurements and improved DFT calculations. In the case of γ-Sn_3N_4, our work is, to our knowledge, the first experimental measurement of its electronic structure and band gap. Although, calculations of the XANES spectra of γ-Sn_3N_4 were previously published [14], our calculations here have better agreement with measurements.

The typical GGA exchange functional (used to calculate the simulated spectra), in most cases, strongly underestimates the electronic band gap. One can see that, compared to the previously predicted band gap values [13,14] where GGA exchange functionals were used, the measured electronic band gaps are ≈ 30% to 60% larger. However, one can predict the electronic band gaps with significantly improved accuracy when the modified Becke-Johnson potential (MBJLDA), implemented within WIEN2K [33], is used instead of the GGA functional. The MBJLDA functional, in the case of *sp* semiconductors does not change the band curvature and only increases the separation between the VB and CB. Since using the MBJLDA functional for core hole calculations is nonphysical, we only use this functional to obtain the correct electronic band gap values. We obtain, through these calculations using a more dense *k*-point grid of 20 × 20 × 20, electronic band gap values of 4.97, 3.59, and 1.61 eV for γ-Si_3N_4, γ-Ge_3N_4, and γ-Sn_3N_4, respectively.

While the binary spinel nitrides presented here are interesting, one can satisfy the needs of a larger range of applications by increasing the variability of the electronic and mechanical properties using solid solutions. Spinel ternary compounds or solid solutions are made by mixing two parent compounds to form ternary spinel nitrides with random occupations of the cation sites. Changing the composition of these materials allows one to engineer the electronic and mechanical properties. Previously, solid solutions of γ-Si_3N_4 and γ-Ge_3N_4 [γ-$(Ge_xSi_{1-x})_3N_4$] have been synthesized and their structure characterized [21]. These solid solutions form in a very symmetric way with the cations retaining their *fcc* arrangement significantly simplifying the crystal structure. The electronic properties of these materials have also been measured and the electronic band gap was found to vary nearly linearly from 3.50 to 4.85 eV [28].

Our simulations of the electronic structures of the binary spinel nitrides are highly accurate, as shown by the agreement between experimental and theoretical electronic structure and band gap. From this, we apply the same method to confirm the electron band gap trend measured for γ-$(Ge_xSi_{1-x})_3N_4$ [28]. We then extend these predictions to include solid solutions of γ-Ge_3N_4 and γ-Sn_3N_4 [γ-$(Sn_{1-x}Ge_x)_3N_4$]. The structures of the solid solutions are modeled using a few simple assumptions. These are that the solid solutions, γ-$(Sn_{1-x}Ge_x)_3N_4$, form in a similar way to γ-$(Ge_xSi_{1-x})_3N_4$ [21]. In particular, we assumed that: (1) the larger cation fills the tetrahedral site before the octahedral site, (2) the lattice constants vary linearly with composition, and (3) the anion bonding parameter varies linearly from the optimized ternary compounds with the filling of tetrahedral sites and octahedral sites. Here, the optimized anion bonding parameters are 0.261 57 and 0.264 13 for γ-$GeSi_2N_4$ and γ-$SnGe_2N_4$, respectively.

Figure 2 shows the theoretical values of the band gaps for the solid solutions, which cover the entire energy range from 1.61 to 4.97 eV. Most the electronic band gaps are predicted to be direct, but a few have slightly smaller indirect electronic band gaps, which are indicated in Fig. 2. It is important to note that the real structure of these materials may be slightly different, since solid solutions, γ-$(Sn_{1-x}Ge_x)_3N_4$, have yet to be synthesized, possibly changing the type of band gap transition with minimum energy. Since our simulation of the end-member compound band gap values using the MBJLDA potential was successful, the calculated band gaps of the solid solutions should be close to their actual values. The previous band gap measurements of γ-$(Ge_xSi_{1-x})_3N_4$ agree with the

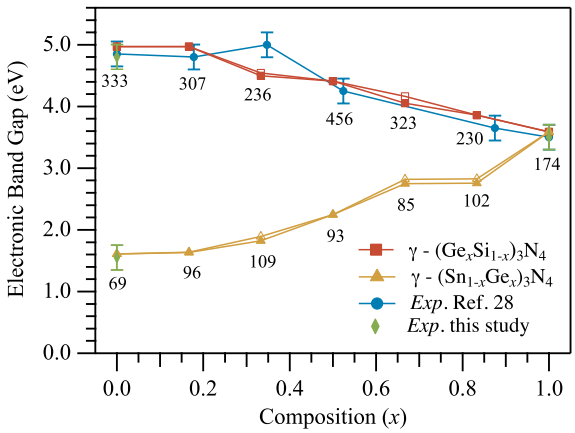

FIG. 2 (color online). The final calculated and measured values for the band gap discussed in this Letter. The direct electronic band gap values are displayed with corresponding open symbols, if the minimum energy transition is indirect. The previous values from Ref. [28] are displayed for comparison. Further, the calculated exciton binding energies, in meV units, are labeled below their respective data points.

calculations presented here within experimental (except for one instance, γ-$GeSi_2N_4$), but has much better agreements than previous calculations [34]. These calculations and measurements showcase the band gap engineering capability of these materials making them appealing for optoelectronic and lighting applications.

According to our results, group 14 spinel nitrides have band gaps spanning the visible wavelength range. However, for a material to be an efficient light emitter, it must not only have a direct electronic band gap, but must also have a large exciton binding energy. If an exciton has a large binding energy, the probability is much greater that it will radiatively decay before the hole and electron can dissociate into free charge carriers. We use the formalism put forth by Ref. [35] to determine the binding energy of a hydrogenic-type exciton quasiparticle. The effective masses and dielectric constants are determined from the band structure of the ground state MBJLDA calculations. Figure 2 shows the exciton binding energy next to the symbols indicating the electronic band gap. While the exciton binding energy is decreased significantly in the γ-$(Sn_{1-x}Ge_x)_3N_4$ solid solutions compared to γ-Si_3N_4, it is still quite large when compared to GaAs ($E_b = 4.20 \pm 0.30$ meV) [36], which has a similar electronic band gap.

We show in this Letter that the solid solutions of spinel-structured group 14 nitrides have tunable electronic band gaps that span the entire visible wavelength region and extend to the near UV and IR. The electronic band gap values for the parent compounds, γ-Si_3N_4, γ-Ge_3N_4, and γ-Sn_3N_4, measured here are 4.8 ± 0.2, 3.5 ± 0.2, and 1.6 ± 0.2 eV, respectively. The calculated exciton binding energy values of γ-Si_3N_4, γ-Ge_3N_4, and γ-Sn_3N_4 are 333, 174, and 69 meV, respectively. The tunability of the electronic band gap and the large exciton binding energies of the spinel-structured group 14 nitride solid solutions suggest that these materials are suitable for optoelectronic applications that require large chemical, thermal, and mechanical stability.

We would like to thank NSERC Canada and the Canadian Research Chair program for their support. XANES measurements were performed at the Canadian Light Source, which is supported by NSERC Canada, NRC Canada, the CIHR, the Province of Saskatchewan, WD Canada, and the University of Saskatchewan. XES measurements used the Advanced Light Source, which is supported by the Office of Basic Energy Sciences of the U.S. DOE under Contract No. DE-AC02-05CH11231. This research has also been enabled by the use of computing resources provided by WestGrid and Compute/Calcul Canada. We also thank H. Jacobs for providing the γ-Sn_3N_4 sample.

*alex.moewes@usask.ca

[1] F. A. Ponce and D. P. Bour, Nature (London) **386**, 351 (1997).
[2] H. Morkoc, S. Strite, G. B. Gao, M. E. Lin, B. Sverdlov, and M. Burns, J. Appl. Phys. **76**, 1363 (1994).
[3] Y.-L. Chang, Y. Song, Z. Wang, M. G. Helander, J. Qiu, L. Chai, Z. Liu, G. D. Scholes, and Z. Lu, Adv. Funct. Mater. **23**, 705 (2013).
[4] B.-G. Kim, C.-G. Zhen, E. J. Jeong, J. Kieffer, and J. Kim, Adv. Funct. Mater. **22**, 1606 (2012).
[5] D. C. Reynolds, D. C. Look, and B. Jogai, Solid State Commun. **99**, 873 (1996).
[6] Y. Kubota, K. Watanabe, O. Tsuda, and T. Taniguchi, Science **317**, 932 (2007).
[7] K. Watanabe, T. Taniguchi, T. Kuroda, and H. Kanda, Appl. Phys. Lett. **89**, 141902 (2006).
[8] A. Zerr, G. Miehe, G. Serghiou, M. Schwarz, E. Kroke, R. Riedel, H. Fueß, P. Kroll, and R. Boehler, Nature (London) **400**, 340 (1999).
[9] G. Serghiou, G. Miehe, O. Tschauner, A. Zerr, and R. Boehler, J. Chem. Phys. **111**, 4659 (1999).
[10] N. Scotti, W. Kockelmann, J. Senker, S. Traßel, and H. Jacobs, Z. Anorg. Allg. Chem. **625**, 1435 (1999).
[11] A. Zerr, R. Riedel, T. Sekine, J. E. Lowther, W.-Y. Ching, and I. Tanaka, Adv. Mater. **18**, 2933 (2006).
[12] S.-D. Mo, L. Ouyang, W. Y. Ching, I. Tanaka, Y. Koyama, and R. Riedel, Phys. Rev. Lett. **83**, 5046 (1999).
[13] W. Y. Ching, S. D. Mo, and L. Ouyang, Phys. Rev. B **63**, 245110 (2001).
[14] W. Y. Ching and P. Rulis, Phys. Rev. B **73**, 045202 (2006).
[15] J. Dong, O. F. Sankey, S. K. Deb, G. Wolf, and P. F. McMillan, Phys. Rev. B **61**, 11979 (2000).
[16] Y. C. Ding, H. P. Zhou, M. Xu, Y. B. Shen, Q. Y. Chen, W.-J. Zhu, and H. L. He, Int. J. Mod. Phys. B **22**, 2157 (2008).
[17] J. Z. Jiang, F. Kragh, D. J. Frost, K. Stahl, and H. Lindelov, J. Phys. Condens. Matter **13**, L515 (2001).
[18] H. L. He, T. Sekine, T. Kobayashi, and K. Kimoto, J. Appl. Phys. **90**, 4403 (2001).
[19] N. Takahashi, K. Terada, and T. Nakamura, J. Mater. Chem. **10**, 2835 (2000).
[20] M. Schwarz, G. Miehe, A. Zerr, E. Kroke, B. T. Poe, H. Fuess, and R. Riedel, Adv. Mater. **12**, 883 (2000).
[21] E. Soignard, P. F. McMillan, and K. Leinenweber, Chem. Mater. **16**, 5344 (2004).
[22] T. Sekine, H. L. He, T. Kobayashi, M. Zhang, and F. F. Xu, Appl. Phys. Lett. **76**, 3706 (2000).
[23] T. Maruyama and T. Morishita, J. Appl. Phys. **77**, 6641 (1995).
[24] M. Chhowalla and H. E. Unalan, Nat. Mater. **4**, 317 (2005).
[25] M. Shemkunas, G. Wolf, K. Leinenweber, and W. Petuskey, J. Am. Ceram. Soc. **85**, 101 (2002).
[26] J. J. Jia, T. A. Callcott, J. Yurkas, A. W. Ellis, F. J. Himpsel, M. G. Samant, J. Stöhr, D. L. Ederer, J. A. Carlisle, E. A. Hudson, L. J. Terminello, D. K. Shuh, and R. C. C. Perera, Rev. Sci. Instrum. **66**, 1394 (1995).
[27] T. Regier, J. Krochak, T. K. Sham, Y. F. Hu, J. Thompson, and R. I. R. Blyth, Nucl. Instrum. Methods Phys. Res., Sect. A **582**, 93 (2007).
[28] T. D. Boyko, E. Bailey, A. Moewes, and P. F. McMillan, Phys. Rev. B **81**, 155207 (2010).
[29] E. Z. Kurmaev, R. G. Wilks, A. Moewes, L. D. Finkelstein, S. N. Shamin, and J. Kuneš, Phys. Rev. B **77**, 165127 (2008).
[30] C. Braun, M. Seibald, S. L. Boerger, O. Oeckler, T. D. Boyko, A. Moewes, G. Miehe, A. Tuecks, and W. Schnick, Chem. Eur. J. **16**, 9646 (2010).

[31] K. Schwarz, P. Blaha, and G. K. H. Madsen, Comput. Phys. Commun. **147**, 71 (2002).
[32] J. P. Perdew, K. Burke, and M. Ernzerhof, Phys. Rev. Lett. **77**, 3865 (1996).
[33] F. Tran and P. Blaha, Phys. Rev. Lett. **102**, 226401 (2009).
[34] J. N. Hart, N. L. Allan, and F. Claeyssens, Phys. Rev. B **84**, 245209 (2011).
[35] N. W. Ashcroft and N. D. Merimin, *Solid State Physics* (Brooks Cole, Belmont, MA, 1976).
[36] S. B. Nam, D. C. Reynolds, C. W. Litton, R. J. Almassy, T. C. Collins, and C. M. Wolfe, Phys. Rev. B **13**, 761 (1976).